[3] M. Zorzi and R. R. Rao, "Error control in multi-layered stacks," in *Proc. IEEE Global Telecommun. Conf.*, Nov. 1997, vol. 3, pp. 1413–1418.
[4] S. Ramakrishna and J. M. Holtzman, "Interaction of TCP and data access control in an integrated voice/data CDMA system," *Mobile Netw. Appl.*, vol. 4, no. 3, pp. 409–417, 1998.
[5] G. Wu, Y. Bai, J. Lai, and A. Ogielski, "Interaction between TCP and RLP in wireless Internet," in *Proc. IEEE Global Telecommun. Conf.*, Nov. 1999, vol. 1b, pp. 661–666.
[6] H. M. Chaskar, T. V. Lakshman, and U. Madhow, "TCP over wireless with link level error control: Analysis and design methodology," *IEEE/ACM Trans. Netw.*, vol. 7, no. 5, pp. 605–615, Oct. 1999.
[7] A. Chockalingam and G. Bao, "Performance of TCP/RLP protocol stack on correlated fading DS-CDMA wireless links," *IEEE Trans. Veh. Technol.*, vol. 49, no. 1, pp. 28–33, Jan. 2000.
[8] F. Lefevre and G. Vivier, "Optimizing UMTS link layer parameters for a TCP connection," in *Proc. IEEE 53rd Veh. Technol. Conf.*, May 2001, vol. 4, pp. 2318–2322.
[9] A. J. McAuley, "Reliable broadband communications using a burst erasure correcting code," in *Proc. ACM SIGCOMM*, 1990, pp. 287–306.
[10] Z. J. Hass and P. Agrawa, "Mobile-TCP: An asymmetric transport protocol design for mobile systems," in *Proc. IEEE Int. Conf. Commun.*, Jun. 1997, vol. 2, pp. 1054–1058.
[11] H. Zheng and J. Boyce, "An improved UDP protocol for video transmission over Internet-to-wireless networks," *IEEE Trans. Multimedia*, vol. 3, no. 3, pp. 356–364, Sep. 2001.
[12] J. Nonnenmacher, E. W. Biersack, and D. Towsley, "Parity-based loss recovery for reliable multicast transmission," *IEEE/ACM Trans. Netw.*, vol. 6, no. 4, pp. 349–361, Aug. 1998.
[13] M. Rossi, M. Zorzi, and F. H. P. Fitzek, "Integration of link layer algorithm and play-out buffer requirements for efficient multicast services in 3G cellular systems," in *Proc. IEEE PIMRC*, Sep. 2004, vol. 3, pp. 2256–2261.
[14] N. Nikaein, H. Labiod, and C. Bonnet, "MA-FEC: A QoS-based adaptive FEC for multicast communication in wireless networks," in *Proc. IEEE Int. Conf. Commun.*, Jun. 2000, vol. 2, pp. 954–958.
[15] J. R. Yee and J. Weldon, "Evaluation of the performance of error-correcting codes on a Gilbert channel," *IEEE Trans. Commun.*, vol. 43, no. 8, pp. 2316–2323, Aug. 1995.
[16] M. Mushkin and I. Bar-David, "Capacity and coding for the Gilbert-Elliott channels," *IEEE Trans. Inf. Theory*, vol. 35, no. 6, pp. 1277–1290, Nov. 1989.
[17] M. J. Miller and S. Lin, "The analysis of some selective-repeat ARQ schemes with finite receiver buffer," *IEEE Trans. Commun.*, vol. COM-29, no. 9, pp. 1307–1315, Sep. 1981.
[18] S. B. Wicker, *Error Control Systems for Digital Communication and Storage*. Englewood Cliffs, NJ: Prentice-Hall, 1995.

Performance Analysis of Two-Branch Space-Time Block-Coded DS-CDMA Systems in Time-Varying Multipath Rayleigh Fading Channels

Ping-Hung Chiang, Ding-Bing Lin, and Hsueh-Jyh Li

***Abstract*—For the two-branch space-time (ST) block-coded direct-sequence code-division multiple-access (DS-CDMA) systems, the impacts of a time-varying multipath channel on the downlink transmission are analyzed. By considering the systems using the random binary spreading code (RBSC) and deterministic binary spreading code (DBSC), the effects of the multipath interference and multiuser interference are included in the analyses of the bit-error rate and bit-error outage. Also, for the performance analysis of the system employing the decision-feedback (DF) detector, the effect of error propagation is taken into account. It is known that enlarging the spreading factor can enhance the interference-rejection ability of a DS-CDMA system and, hence, can improve the performance. However, it also lengthens the symbol duration and, thus, stiffens the diversity penalty resulting from the channel variation within an ST-code-word duration. Thus, a moderate spreading factor should be chosen. In this paper, for the RBSC system using the simple-maximum-likelihood (SML) detector, we derive an optimum spreading factor that is optimum in the minimum-error-probability sense. Numerical results have revealed that the derived optimum spreading factor is a good estimate of the ones for the DBSC systems using the SML, zero-forcing, and DF detectors. Therefore, it is very useful for system designers in determining the system parameters.**

***Index Terms*—Bit-error outage (BEO), direct-sequence code-division multiple access (DS-CDMA), multipath interference (MPI), multiuser interference (MUI), space-time block coding (STBC), transmit diversity.**

I. Introduction

Space-time block coding (STBC), which is an effective transmit-diversity technique, was first proposed by Alamouti [1] for flat fading channels Assuming the channel being constant over an ST-code-word duration (i.e., two symbol durations) and the channel state information (CSI) being known at the receiver, he showed that the proposed two-input–single-output (2ISO) diversity system utilizing a simple-maximum-likelihood (SML) detector can obtain the full-diversity advantage. However, it suffers from a diversity penalty when the quasi-static (QS) channel assumption is dropped. Recently, the impacts of a time-varying channel on the Alamouti scheme were investigated [2]–[4]. Vielmon *et al.* [2] proposed three detectors to enhance the system robustness for rapid channel variation. These detectors are the zero-forcing (ZF), decision-feedback (DF), and joint-maximum-likelihood (JML) detectors. The ZF and DF detectors are of suboptimum performances but of moderate complexities, while the JML detector is of the optimum performance but of the highest complexity. Considering the CSI being not available at the receiver, Liu *et al.* [3] proposed a channel-tracking method using the Kalman filter to track

Manuscript received June 14, 2005; revised February 2, 2006 and April 20, 2006. This work was supported in part by the National Science Council, Republic of China, under Grant NSC 92-2219-E-002-010 and in part by the MOE Program for promoting academic excellence of universities under Grant 89E-FA06-2-4-7. The review of this paper was coordinated by Prof. L. H.-J. Lampe.

P.-H. Chiang and H.-J. Li are with the Graduate Institute of Communication Engineering, National Taiwan University, Taipei 10617, Taiwan, R.O.C. (e-mail: d1942011@ee.ntu.edu.tw; hjli@ew.ee.ntu.edu.tw).

D.-B. Lin is with the Department of Electronic Engineering, National Taipei University of Technology, Taipei 10617, Taiwan, R.O.C. (e-mail: dblin@en.ntut.edu.tw).

Digital Object Identifier 10.1109/TVT.2007.891424

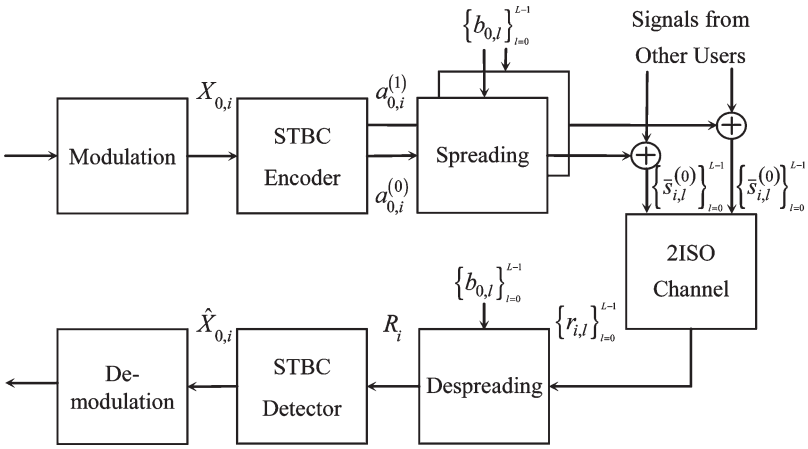

Fig. 1. Discrete-time baseband-equivalent-system model.

the temporal channel variation. The proposed receiver introduced with the SML and JML detectors can perform the channel tracking and data detection iteratively. It is noteworthy that the extension of their work based on the DF detector was discussed in [4].

It is well-known that the interferences degrade the performance of a direct-sequence code-division multiple-access (DS-CDMA) system in multipath fading channels [5]. These interferences are 1) the multipath interferences (MPI), consisting of the intersymbol interference (ISI) and the interpath interference (IPI), due to multipath propagation and 2) the multiuser interference (MUI) from other active users. To improve the downlink transmission without drastically increasing the receiver complexity, the Alamouti scheme was adopted in the third-generation (3G) universal-mobile-telecommunication-system (UMTS) standard [6]. Please refer to [7] and [8] for the tutorial reviews of the applications of the Alamouti scheme and the other transmit-diversity schemes in the 3G-CDMA systems.

For the downlink transmission, the STBC-DS-CDMA system employing the Alamouti scheme has been discussed by many researchers. Bjerke *et al.* [9] considered the combinations of the Alamouti scheme and various receive diversity schemes and derived their bit-error-rate (BER) expressions by assuming the channel being QS. Also, they assumed that the despreading operation is perfect, and hence, the effects of the MPI and MUI were not taken into account. In [10], the authors analyzed the effect of imperfect channel estimation with the QS channel assumption. Assuming the spreading code being random, they studied the effects of the IPI and MUI but ignored the one of ISI. In [11], the authors considered the SML and JML detectors and theoretically evaluated the performance of the system with noisy channel estimates in time-varying channels. However, as in [9], the effects of the MPI and MUI were not taken into consideration.

In this paper, assuming the CSI being available at the receiver, we analyze the impacts of a time-varying multipath channel on the downlink 2ISO STBC-DS-CDMA systems employing the SML, ZF, DF, and JML detectors. By considering the systems using the random binary spreading code (RBSC) and deterministic binary spreading code (DBSC), named the RBSC and DBSC systems, respectively, the effects of the MPI and MUI are included in the analyses of the BER and bit-error outage (BEO), i.e., outage probability [12]. It is known that enlarging the spreading factor (i.e., the number of chips per symbol) can enhance the interference-rejection ability of a DS-CDMA system and, hence, can improve the performance. However, it also lengthens the symbol duration and, thus, stiffens the diversity penalty resulting from the channel variation within an ST-code-word duration. Thereupon, a moderate spreading factor should be chosen according to a set of system and channel parameters, and our objective is to develop a method for determining such a spreading factor. The major novelties of this paper are listed as follows.

1) For both RBSC and DBSC systems, the variances of the IPI, ISI, and MUI are derived. In the derivation, the channel is assumed to be constant within a chip duration only, and the ISI is assumed to be the contribution of the multiple previous symbols. These two assumptions make our derivation more practical and general than the ones in [7]–[11].
2) For the system employing the DF detector, the effect of error propagation is included in the derived BER expression. This was not considered in [2] and [13].
3) For the RBSC system employing the SML detector, an optimum spreading factor that is optimum in the minimum-error-probability sense is derived.

The rest of this paper is organized as follows. In Section II, the system and channel models are described. Then, various strategies for the receiver design are presented in Section III, and their BER expressions are given in Section IV. Also, the derivation of the optimum spreading factor is provided in Section V. Numerical results are shown in Section VI, while conclusions are drawn in Section VII.

II. System and Channel Models

As shown in Fig. 1, we consider the STBC-DS-CDMA system, equipped with two transmit antennas at the base station and one receive antenna at the mobile terminal, in the synchronous downlink transmission.

A. Transmitter Model

Let $X_{k,i}$ denote the information symbol of the kth user in the ith symbol interval. Also, let T_S and E_S represent the symbol duration and the symbol energy, respectively. At the transmitter, a pair of information symbols $\{X_{k,i}, i = 2q+0, 2q+1\}$ for the qth ST-code-word duration is first ST block-encoded via [1]

$$\begin{matrix}\text{Space} \rightarrow \\ \text{Time} \downarrow\end{matrix} \begin{bmatrix} a_{k,2q+0}^{(0)} & a_{k,2q+0}^{(1)} \\ a_{k,2q+1}^{(0)} & a_{k,2q+1}^{(1)} \end{bmatrix} = \begin{bmatrix} X_{k,2q+0} & X_{k,2q+1} \\ -X_{k,2q+1}^{*} & X_{k,2q+0}^{*} \end{bmatrix} \quad (1)$$

where $\{a_{k,i}^{(g)}, i = 2q+0, 2q+1\}$ is a pair of channel symbols to be transmitted from the gth transmit antenna. Let $\{b_{k,l}, 0 \le l \le L-1\}$ be the spreading sequence of the kth user, where L is the spreading factor. Also, $b_{k,l}$ takes on the values of $\pm 1/\sqrt{L}$ with equal probability for RBSC or according to the assignment of the code book for DBSC. Considering short code spreading (i.e., $T_S = LT_C$ and T_C being the

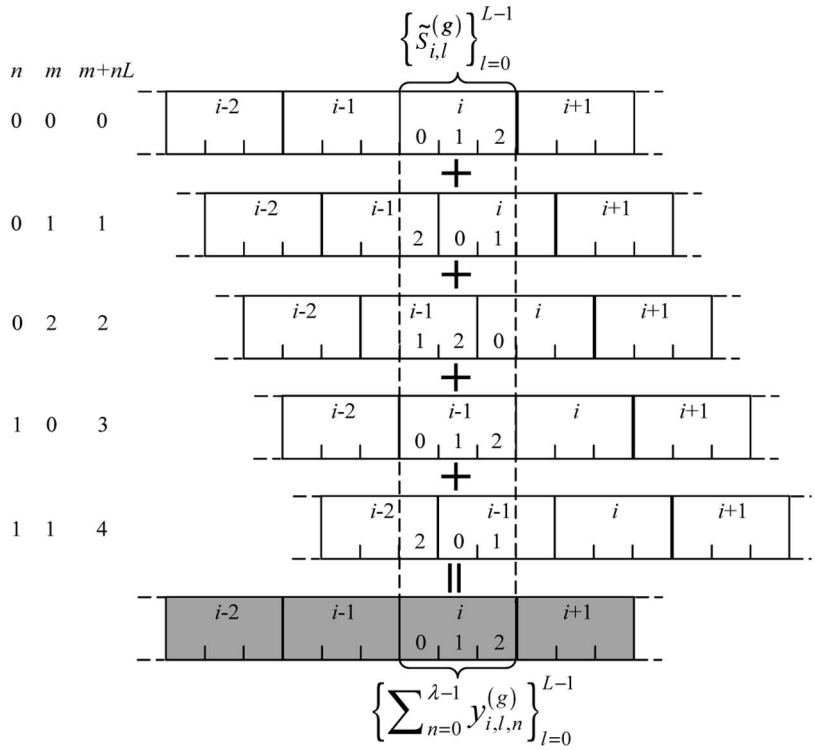

Fig. 2. Graphical illustration of the received signals for $M = 5$, $L = 3$, and $N = \lambda = 2$.

chip duration or the reciprocal of the system bandwidth), we write the transmitted sequence as

$$\tilde{s}_{i,l}^{(g)} = \sum_{k=0}^{K-1} a_{k,i}^{(g)} b_{k,l}, \qquad \text{for } 0 \le l \le L-1 \tag{2}$$

where K is the number of users. Provided $\tilde{s}_{i,l}^{(g)} = 0$ for $l < 0$ and $l \ge L$, the total transmitted baseband sequence from the gth transmit antenna is

$$s_l^{(g)} = \sum_{i=-\infty}^{\infty} \tilde{s}_{i,l-iL}^{(g)}. \tag{3}$$

B. Channel Model

In this paper, we employ the chip-spaced tapped-delay-line (TDL) channel model [14] (i.e., a TDL with a fixed tap spacing T_C) and assume that the channel from the gth transmit antenna to the receive antenna consists of M discrete paths, expressed as a set of tap coefficients $\{h_{m,l}^{(g)}, 0 \le m \le M-1\}$. It is assumed that the two channels, corresponding to two transmit antennas, experience independently and identically distributed (i.i.d.) Rayleigh fading and have an identical power-delay profile. More specifically, $h_{m,l}^{(g)} \sim \mathcal{CN}(0, \sigma_m^2)$ for $g = 0, 1$, where σ_m^2 is the fading power of the mth path complying with the constraint $\sum_{m=0}^{M-1} \sigma_m^2 = 1$. Also, the channel is assumed to be constant within a chip duration only. Subsequently, a temporal rearrangement of the tap coefficients is defined as $h_{m,i,l}^{(g)} \triangleq h_{m,iL+l}^{(g)}$, which will be used later in the receiver model (see Section II-C). For the wide-sense-stationary-uncorrelated-scattering (US) channel with classical Doppler spectrum, the correlation between the rearranged tap coefficients is expressed as [14]

$$E\left[h_{m,i,l}^{(g)} h_{m',i',l'}^{(g')*}\right] = \sigma_m^2 J_0\left\{2\pi f_D T_C\left[(i-i')L + (l-l')\right]\right\} \delta_{mm'} \delta_{gg'} \tag{4}$$

where $J_0(\cdot)$ is the zeroth-order Bessel function of the first kind, f_D is the maximum Doppler frequency, and δ_{ij} is the Kronecker delta.

C. Receiver Model

Provided that the receiver can achieve perfect chip-timing synchronization and power control, the received baseband sequence of the desired user, denoted by the zeroth user, can be expressed as

$$\begin{aligned} r_l &= \sum_{g=0}^{1} \sum_{m=0}^{M-1} h_{m,l}^{(g)} s_{l-m}^{(g)} + z_l \\ &= \sum_{g=0}^{1} \sum_{i=-\infty}^{\infty} \sum_{m=0}^{M-1} h_{m,l}^{(g)} \tilde{s}_{i,l-m-iL}^{(g)} + z_l \end{aligned} \tag{5}$$

where $z_l \sim \mathcal{CN}(0, 2N_0)$ is the additive white Gaussian noise. The factor 2 is due to the sharing of the transmitting power for two antennas. To quantify the ISI due to multipath propagation, the number of previous symbols causing the ISI is defined as $N \triangleq \lceil (M-1)/L \rceil$, where the function $\lceil x \rceil$ gives the smallest integer larger than or equal to x. Also, we define $\lambda \triangleq \lceil M/L \rceil$ and

$$\kappa(n) \triangleq \begin{cases} L, & \text{if } M = \lambda L \text{ and } 0 \le n \le \lambda - 1 \\ L, & \text{if } M \ne \lambda L \text{ and } 0 \le n \le \lambda - 2 \\ ((M))_L, & \text{if } M \ne \lambda L \text{ and } n = \lambda - 1 \end{cases} \tag{6}$$

where $((\cdot))_L$ denotes the modulo-L operation. It can be shown that λ and N are related as

$$\lambda = \begin{cases} N, & \text{if } ((M))_L \ne 1 \\ N+1, & \text{if} ((M))_L = 1 \,. \end{cases} \tag{7}$$

Then, as shown in Fig. 2, rearranging r_l symbol by symbol as $r_{i,l} \triangleq r_{iL+l}$ yields

$$r_{i,l} = \sum_{g=0}^{1} \sum_{n=0}^{\lambda-1} y_{i,l,n}^{(g)} + z_{i,l}, \qquad \text{for} \quad 0 \le l \le L-1 \tag{8}$$

where $z_{i,l} \triangleq z_{iL+l}$ is the rearranged noise and $y_{i,l,n}^{(g)}$ is the noise-free received signal given by (9), shown at the bottom of the page. Without loss of generality, the zeroth path of the multipath channel is assumed to have the largest fading power. Thus, the code-matched filter performs despreading with respect to the zeroth path and produces the signal for the ith symbol duration as

$$R_i = \sum_{l=0}^{L-1} r_{i,l} b_{0,l} = \sum_{g=0}^{1} \left(H_i^{(g)} a_{0,i}^{(g)} + P_i^{(g)} + S_i^{(g)} + U_i^{(g)} \right) + Z_i \quad (10)$$

where $H_i^{(g)}$, $P_i^{(g)}$, $S_i^{(g)}$, $U_i^{(g)}$, and Z_i are the multiplicative distortion (MD), IPI, ISI, MUI, and noise, respectively. They are given by

$$H_i^{(g)} = \frac{1}{L} \sum_{l=0}^{L-1} h_{0,i,l}^{(g)} \quad (11)$$

$$P_i^{(g)} = a_{0,i}^{(g)} \sum_{m=1}^{\kappa(0)-1} \sum_{l=m}^{L-1} h_{m,i,l}^{(g)} b_{0,l-m} b_{0,l} \quad (12)$$

$$S_i^{(g)} = \sum_{n=1}^{\lambda-1} a_{0,i-n}^{(g)} \sum_{m=0}^{\kappa(n)-1} \sum_{l=m}^{L-1} h_{m+nL,i,l}^{(g)} b_{0,l-m} b_{0,l} + \sum_{n=0}^{\lambda-1} a_{0,i-n-1}^{(g)} \sum_{m=1}^{\kappa(n)-1} \sum_{l=0}^{m-1} h_{m+nL,i,l}^{(g)} b_{0,l-m+L} b_{0,l} \quad (13)$$

$$U_i^{(g)} = \sum_{k=1}^{K-1} \sum_{n=0}^{\lambda-1} \left(a_{k,i-n}^{(g)} \sum_{m=0}^{\kappa(n)-1} \sum_{l=m}^{L-1} h_{m+nL,i,l}^{(g)} b_{k,l-m} b_{0,l} + a_{k,i-n-1}^{(g)} \sum_{m=1}^{\kappa(n)-1} \sum_{l=0}^{m-1} h_{m+nL,i,l}^{(g)} b_{k,l-m+L} b_{0,l} \right) \quad (14)$$

$$Z_i = \sum_{l=0}^{L-1} z_{i,l} b_{0,l} \quad (15)$$

where (12)–(14) are derived by changing the order of summations and rearranging the resultant terms.

Subsequently, some statistical properties regarding the random variables (RVs) given in (11)–(15) are specified as follows.

1) The channel symbols $\{a_{k,i}^{(g)}, 0 \le k \le K-1 \text{ and } -\infty \le i \le \infty\}$ are i.i.d. and have zero mean and variance E_S, provided that $\{X_{k,i}, 0 \le k \le K-1 \text{ and } -\infty \le i \le \infty\}$ are i.i.d. information symbols having zero mean and variance E_S. This can be verified from (1).
2) The tap coefficients $\{h_{m,i,l}^{(g)}, 0 \le m \le M-1\}$ are mutually uncorrelated due to the assumption of US.
3) The MD $H_i^{(g)}$ is distributed as $\mathcal{CN}(0, \sigma_H^2)$, since it is a linear combination of zero-mean complex Gaussian RVs. To characterize the channel variation, its normalized correlation of adjacent symbol durations, which is denoted by ρ_t, is used. See Appendix A for the expressions of σ_H^2 and ρ_t.
4) The noise Z_i is distributed as $\mathcal{CN}(0, 2N_0)$ for both RBSC and DBSC systems.
5) The interferences, including $P_i^{(g)}$, $S_i^{(g)}$, and $U_i^{(g)}$, are zero-mean RVs and mutually uncorrelated. Also, they are uncorrelated to the MD $H_i^{(g)}$ and the noise Z_i.

According to 5), it is reasonable to model the interferences as Gaussian RVs. Since independent Gaussian noise results in the smallest capacity, the performance bound can be achieved [15]. Indeed, (10) can be rewritten as

$$R_i = \sum_{g=0}^{1} H_i^{(g)} a_{0,i}^{(g)} + W_i \quad (16)$$

where $W_i \sim \mathcal{CN}(0, \sigma_W^2)$ is given by

$$W_i = \sum_{g=0}^{1} \left(P_i^{(g)} + S_i^{(g)} + U_i^{(g)} \right) + Z_i. \quad (17)$$

Here, $\sigma_W^2 = 2(\sigma_P^2 + \sigma_S^2 + \sigma_U^2 + N_0)$, where σ_P^2, σ_S^2, and σ_U^2 represent the variances of $P_i^{(g)}$, $S_i^{(g)}$, and $U_i^{(g)}$, respectively. Please refer to Appendices B and C for the derivations of σ_P^2, σ_S^2, and σ_U^2.

III. Strategies for Receiver Design

In this section, assuming the CSI being known perfectly at the receiver, we introduce four strategies for the receiver design, including the JML, SML, ZF, and DF detectors and give a remark on their computational complexities. According to (1) and (16), the signal model for detecting the qth ST code word is

$$\mathbf{r} = \mathbf{H}\mathbf{x} + \mathbf{w}$$

$$\begin{bmatrix} R_{2q+0} \\ R_{2q+1}^* \end{bmatrix} = \begin{bmatrix} H_{2q+0}^{(0)} & H_{2q+0}^{(1)} \\ H_{2q+1}^{(1)^*} & -H_{2q+1}^{(0)^*} \end{bmatrix} \begin{bmatrix} X_{2q+0} \\ X_{2q+1} \end{bmatrix} + \begin{bmatrix} W_{2q+0} \\ W_{2q+1}^* \end{bmatrix} \quad (18)$$

where the subscript zero of the information symbol $X_{0,i}$ is omitted for simplicity.

A. JML Detector

From (18), since the noise is white, the JML detector makes decision about $\mathbf{x}$ via [13, eq. (23)]

$$\hat{\mathbf{x}}^{\mathrm{JML}} = \arg\min_{\mathbf{x}} \left\{ \|\mathbf{r} - \mathbf{H}\mathbf{x}\|^2 \right\}. \quad (19)$$

Let the cascade of $\mathbf{H}$ and its matched filter be

$$\tilde{\mathbf{H}} = \mathbf{H}^{\mathrm{H}}\mathbf{H} = \begin{bmatrix} \alpha_0 & \beta \\ \beta^* & \alpha_1 \end{bmatrix} \quad (20)$$

where $\alpha_0 = |H_{2q+0}^{(0)}|^2 + |H_{2q+1}^{(1)}|^2$, $\alpha_1 = |H_{2q+0}^{(1)}|^2 + |H_{2q+1}^{(0)}|^2$, and $\beta = H_{2q+0}^{(0)^*} H_{2q+0}^{(1)} - H_{2q+1}^{(0)*} H_{2q+1}^{(1)}$. Since $\tilde{\mathbf{H}}$ is Hermitian, it has a

$$y_{i,l,n}^{(g)} = \begin{cases} \sum_{m=0}^{l} h_{m+nL,i,l}^{(g)} \tilde{s}_{i-n,l-m}^{(g)} + \sum_{m=l+1}^{\kappa(n)-1} h_{m+nL,i,l}^{(g)} \tilde{s}_{i-n-1,l-m+L}^{(g)}, & \text{if } 0 \le l \le \kappa(n)-2 \\ \sum_{m=0}^{\kappa(n)-1} h_{m+nL,i,l}^{(g)} \tilde{s}_{i-n,l-m}^{(g)}, & \text{if } \kappa(n)-1 \le l \le L-1 \end{cases} \quad (9)$$

unique Cholesky factorization as $\tilde{\mathbf{H}} = \mathbf{G}^H\mathbf{G}$, where

$$\mathbf{G} = \begin{bmatrix} \xi\alpha_1^{-1/2} & 0 \\ \beta^*\alpha_1^{-1/2} & \alpha_1^{1/2} \end{bmatrix} \tag{21}$$

is a lower triangular matrix and $\xi = |H_{2q+0}^{(0)}H_{2q+1}^{(0)^*} + H_{2q+0}^{(1)}H_{2q+1}^{(1)*}|$. Then, applying whiten-matched filtering on the received ST code word yields [13, eq. (30)]

$$\mathbf{r}_W = \mathbf{C}_W\mathbf{r} = \mathbf{G}\mathbf{x} + \mathbf{w}_W \tag{22}$$

where $\mathbf{r}_W \triangleq [R_{W,0} \quad R_{W,1}]^{\mathrm{T}}$, $\mathbf{C}_W = \mathbf{G}^{-H}\mathbf{H}^H$, and $\mathbf{w}_W = \mathbf{C}_W\mathbf{w} \triangleq [W_{W,0} \quad W_{W,1}]^{\mathrm{T}}$. Since the noise $\mathbf{w}_W$ is still white, the JML detector is now equivalent to [13, eq. (31)]

$$\hat{\mathbf{x}}^{\mathrm{JML}} = \arg\min_{\mathbf{x}} \left\{ \|\mathbf{r}_W - \mathbf{G}\mathbf{x}\|^2 \right\}. \tag{23}$$

B. SML Detector

Performing ST-matched filtering on the received ST code word results in [13, eq. (24)]

$$\mathbf{r}_M = \mathbf{C}_M\mathbf{r} = \mathbf{H}_M\mathbf{x} + \mathbf{w}_M \tag{24}$$

where $\mathbf{r}_M \triangleq [R_{M,0} \quad R_{M,1}]^{\mathrm{T}}$, $\mathbf{C}_M = \mathbf{A}_M\mathbf{H}^H$, $\mathbf{H}_M = \mathbf{A}_M\tilde{\mathbf{H}}$, $\mathbf{w}_M = \mathbf{C}_M\mathbf{w} \triangleq [W_{M,0}\ W_{M,1}]^{\mathrm{T}}$, and $\mathbf{A}_M = \mathrm{diag}\{\alpha_0^{-1/2}, \alpha_1^{-1/2}\}$. From (24), without considering the correlation of the noise $\mathbf{w}_M$ and the crosstalks (i.e., the off-diagonal terms of $\mathbf{H}_M$), the SML detector simply obtains the decisions about X_{2q+0} and X_{2q+1} via [13, eq. (32)]

$$\hat{X}_{2q+p}^{\mathrm{SML}} = \arg\min_{X} \left\{ \left| R_{M,p} - \alpha_P^{1/2}X \right|^2 \right\}, \qquad \text{for } p = 0, 1. \tag{25}$$

C. ZF Detector

From (24), the ZF detector forces the crosstalks to zero through [13, eq. (33)]

$$\mathbf{r}_Z = \mathbf{C}_Z\mathbf{r}_M = \mathbf{A}_Z\mathbf{x} + \mathbf{w}_Z \tag{26}$$

where $\mathbf{r}_Z \triangleq [R_{Z,0} \quad R_{Z,1}]^{\mathrm{T}}$, $\mathbf{C}_Z = \mathbf{A}_Z\mathbf{H}_M^{-1}$, $\mathbf{w}_Z = \mathbf{C}_Z\mathbf{w}_M \triangleq [W_{Z,0}\ W_{Z,1}]^{\mathrm{T}}$, and $\mathbf{A}_Z = \mathrm{diag}\{\xi\alpha_1^{-1/2}, \xi\alpha_0^{-1/2}\} \triangleq \mathrm{diag}\{A_{Z,0}, A_{Z,1}\}$. Consequently, the ZF detector can separately make decisions about X_{2q+0} and X_{2q+1} via [13, eq. (35)]

$$\hat{X}_{2q+p}^{\mathrm{ZF}} = \arg\min_{X} \left\{ |R_{Z,p} - A_{Z,p}X|^2 \right\}, \qquad \text{for } p = 0, 1. \tag{27}$$

D. DF Detector

From (22), the DF detector feeds back the decision about X_{2q+0} to help make a decision about X_{2q+1}, namely [13, eq. (36)]

$$\begin{cases} \hat{X}_{2q+0}^{\mathrm{DF}} = \arg\min_{X} \left\{ \left| R_{W,0} - \xi\alpha_1^{-1/2}X \right|^2 \right\} \\ \hat{X}_{2q+1}^{\mathrm{DF}} = \arg\min_{X} \left\{ \left| \widehat{R}_{W,1} - \alpha_1^{1/2}X \right|^2 \right\} \end{cases} \tag{28}$$

where $\widehat{R}_{W,1} \triangleq R_{W,1} - \beta^*\alpha_1^{-1/2}\hat{X}_{2q+0}^{DF}$ is the decision statistic after crosstalk cancellation.

IV. Performance Analysis

For binary phase-shift keying (BPSK), we evaluate the theoretical BERs of the 2ISO STBC-DS-CDMA system in time-varying multipath Rayleigh fading channels. First, the effective signal-to-noise ratios (ESNRs), i.e., average signal-to-interference-plus-noise ratios, are determined according to the variances of the MD and the interferences. Then, the theoretical BERs of the JML, SML, and ZF detectors are obtained by substituting the ESNRs into the BER expressions given in [2]. Noteworthily, for the DF detector, we derive its BER expression being able to reflect the effect of error propagation. By using the derived ESNRs and BERs and following the same steps given in [13, Sec. VI-A], one can also evaluate the theoretical BEOs easily. Finally, a remark on computational complexities of all detectors is provided.

A. JML Detector

Since the JML detector is robust to the crosstalk resulting from the channel variation within an ST-code-word duration, we can treat its performance for the QS condition (i.e., $H_{2q+0}^{(g)} = H_{2q+1}^{(g)}$, for $g = 0, 1$) as a lower bound. Under this condition, the first component of (22) is reduced to

$$R_{W,0} = \alpha_0^{1/2}X_{2q+0} + W_{W,0}. \tag{29}$$

According to (29), the BER of the JML detector is given as [2, eq. (16)]

$$P_b^{\mathrm{JML}} \geq \frac{1}{4}\left(1 - \sqrt{\frac{\bar{\gamma}}{2+\bar{\gamma}}}\right)^2\left(2 + \sqrt{\frac{\bar{\gamma}}{2+\bar{\gamma}}}\right) \triangleq f_1(\bar{\gamma}) \tag{30}$$

where the ESNR is $\bar{\gamma} = 2\sigma_H^2E_S/\sigma_W^2$.

B. SML Detector

The first component of (24) is

$$R_{M,0} = \alpha_0^{1/2}X_{2q+0} + \beta\alpha_0^{-1/2}X_{2q+1} + W_{M,0}. \tag{31}$$

In [13, App.], we showed that the crosstalk $\beta\alpha_0^{-1/2}X_{2q+1}$ is a zero-mean RV and has variance $\sigma_H^2E_S(1-\rho_t^2)$. By assuming that the crosstalk is Gaussian distributed, the BER of the SML detector is derived as [13, eq. (43)]

$$P_b^{\mathrm{SML}} = f_1(\bar{\gamma}_{\mathrm{SML}}) \tag{32}$$

where the ESNR is $\bar{\gamma}_{\mathrm{SML}} = 2\sigma_H^2E_S/[\sigma_H^2E_S(1-\rho_t^2) + \sigma_W^2]$.

C. ZF Detector

According to the first component of (26), which is given as

$$R_{Z,0} = \xi\alpha_1^{-1/2}X_{2q+0} + W_{Z,0} \tag{33}$$

the BER of the ZF detector is derived as [2, eq. (30)]

$$\begin{aligned} P_b^{\mathrm{ZF}} &= \left(1-\rho_t^2\right)\left[\frac{1}{2}\left(1 - \sqrt{\frac{\bar{\gamma}}{2+\bar{\gamma}}}\right)\right] \\ &\quad + \rho_t^2\left[\frac{1}{4}\left(1 - \sqrt{\frac{\bar{\gamma}}{2+\bar{\gamma}}}\right)^2\left(2 + \sqrt{\frac{\bar{\gamma}}{2+\bar{\gamma}}}\right)\right] \\ &\triangleq f_2(\bar{\gamma}). \end{aligned} \tag{34}$$

D. DF Detector

Observing from (22) and (33), one can find that $R_{W,0}$ has the same form as $R_{Z,0}$. Thus, we can write the BER of the DF detector for the first symbol X_{2q+0} as

$$P_{b,0}^{\mathrm{DF}} = P_b^{\mathrm{ZF}} = f_2(\bar{\gamma}). \tag{35}$$

On the other hand, the BER of the DF detector for the second symbol X_{2q+1} is computed via

$$P_{b,1}^{\mathrm{DF}} = P_{b,1|\mathrm{Correct}}^{\mathrm{DF}} P_{\mathrm{Correct}} + P_{b,1|\mathrm{Incorrect}}^{\mathrm{DF}} P_{\mathrm{Incorrect}} \tag{36}$$

where $P_{b,1|\mathrm{Correct}}^{\mathrm{DF}}$ and $P_{b,1|\mathrm{Incorrect}}^{\mathrm{DF}}$ are the error probabilities for the second symbol given, respectively, correct and incorrect feedback decisions. Also, the probability of incorrect feedback decision is

$$P_{\mathrm{Incorrect}} = \Pr\left\{\hat{X}_{2q+0}^{\mathrm{DF}} \neq X_{2q+0}^{\mathrm{DF}}\right\} = P_{b,0}^{\mathrm{DF}} = f_2(\bar{\gamma}) \tag{37}$$

and hence, the probability of correct feedback decision is

$$P_{\mathrm{Correct}} = 1 - P_{\mathrm{Incorrect}} = 1 - f_2(\bar{\gamma}). \tag{38}$$

If the feedback decision $\hat{X}_{2q+0}^{\mathrm{DF}}$ is correct, $\widehat{R}_{W,1}$ is of the same form as (29), and thus, we have $P_{b,1|\mathrm{Correct}}^{\mathrm{DF}} = f_1(\bar{\gamma})$. However, if $\hat{X}_{2q+0}^{\mathrm{DF}}$ is incorrect, $\widehat{R}_{W,1}$ becomes

$$\widehat{R}_{W,1} = \alpha_1^{1/2} X_{2q+1}^{\mathrm{DF}} + \beta^* \alpha_1^{-1/2} \varepsilon_{2q+0} + W_{W,1} \tag{39}$$

where $\varepsilon_{2i+0} \triangleq X_{2q+0} - \hat{X}_{2q+0}^{\mathrm{DF}}$, for BPSK takes on the values of $\pm 2\sqrt{E_S}$ with equal probability. Since the error term $\beta^* \alpha_1^{-1/2} \varepsilon_{2q+0}$ has the same form as the crosstalk $\beta \alpha_1^{-1/2} X_{2q+0}$, we can assume that its distribution is $\mathcal{CN}(0, 4\sigma_H^2 E_S(1-\rho_t^2))$. Then, since (39) is of the same form as (31), one can obtain $P_{b,1|\mathrm{Incorrect}}^{\mathrm{DF}} = f_1(\bar{\gamma}_{\mathrm{DF}})$, where the ESNR is $\bar{\gamma}_{\mathrm{DF}} = 2\sigma_H^2 E_S / [4\sigma_H^2 E_S(1-\rho_t^2) + \sigma_W^2]$. Finally, the BER of the DF detector can be calculated via

$$\begin{aligned} P_b^{\mathrm{DF}} &= \frac{1}{2}\left(P_{b,0}^{\mathrm{DF}} + P_{b,1}^{\mathrm{DF}}\right) \\ &= \frac{1}{2}\left\{f_2(\bar{\gamma}) + f_1(\bar{\gamma})\left[1 - f_2(\bar{\gamma})\right] + f_1(\bar{\gamma}_{\mathrm{DF}}) f_2(\bar{\gamma})\right\}. \end{aligned} \tag{40}$$

E. Remark on Computational Complexity

As shown in (19), the JML detector detects two symbols jointly and, hence, has the highest computational complexity, especially when the constellation size of the information symbol is large. As compared to the SML detector, the ZF detector requires the additional computation for matrix inversion while the DF detector requires the ones for both Cholesky factorization and matrix inversion. Therefore, the ZF and DF detectors have higher computational complexities than the SML detector. Moreover, the DF detector has higher computational complexity than the ZF detector as a result of crosstalk cancellation. As compared to the JML and SML detectors, the ZF and DF detectors have suboptimum performances but moderate computational complexities. Indeed, we recommend the ZF and DF detectors for practical implementations.

V. Optimum Spreading Factor

In this section, the optimum spreading factor for RBSC system using the SML detector is derived. Here, we define the sum of the powers of the interferences and crosstalk as

$$\sigma_{I,\mathrm{SML}}^2 = 2\left(\sigma_P^2 + \sigma_S^2 + \sigma_U^2\right) + \sigma_H^2 E_S\left(1 - \rho_t^2\right). \tag{41}$$

From (31), the ESNR for the SML detector can then be rewritten as

$$\bar{\gamma}_{\mathrm{SML}} = \frac{2\sigma_H^2 E_S}{\sigma_{I,\mathrm{SML}}^2 + 2N_0}. \tag{42}$$

Now, we derive the optimum spreading factor for the case of $M \leq L$ first. The derivation for the case of $M > L$ will be given later. For RBSC, according to (49) and (55), by using $J_0(x) \approx 1 - 0.25\ x^2$ [16, eq. (8.441-1)] and $L \gg 1$, (41) can be approximated as

$$\sigma_{I,\mathrm{SML}}^2 = E_S\left[\frac{2}{L}\left(\sum_{m=1}^{M-1}\sigma_m^2 + K - 1\right) + \frac{7L^2}{3}(\pi f_D T_C)^2 \sigma_0^2\right] \tag{43}$$

of which the high-order terms are ignored. Since (43) is a convex function of L over $(0, \infty)$, an optimum spreading factor $L_{\mathrm{opt}}^{\mathrm{SML}}$ for minimizing $\sigma_{I,\mathrm{SML}}^2$ can be found. From (32) and (42), it is obvious that P_b^{SML} is a monotone increasing function of $\sigma_{I,\mathrm{SML}}^2$. Thus, $L_{\mathrm{opt}}^{\mathrm{SML}}$ is also optimum in the sense of minimizing P_b^{SML}. Since $\sigma_{I,\mathrm{SML}}^2$ is convex, one can obtain $L_{\mathrm{opt}}^{\mathrm{SML}}$ by the following steps. First, solving

$$\left.\frac{\partial}{\partial L}\sigma_{I,\mathrm{SML}}^2\right|_{L=L_{\mathrm{opt}}} = 0 \tag{44}$$

yields

$$L_{\mathrm{opt}} = \left(\frac{3}{7} \cdot \frac{\sum_{m=1}^{M-1}\sigma_m^2 + K - 1}{(\pi f_D T_C)^2 \sigma_0^2}\right)^{1/3}. \tag{45}$$

Second, according to L_{opt}, one can determine L_{opt}^- and L_{opt}^+ from all possible spreading factors. For instance, if $L_{\mathrm{opt}} = 52.13$ and the set of possible spreading factors is $\{1, 3, 7, 15, 31, 63, \ldots\}$, then $L_{\mathrm{opt}}^- = 31$ and $L_{\mathrm{opt}}^+ = 63$. Finally, the optimum spreading factor $L_{\mathrm{opt}}^{\mathrm{SML}}$ is determined via

$$L_{\mathrm{opt}}^{\mathrm{SML}} = \underset{L_{\mathrm{opt}}^-, L_{\mathrm{opt}}^+}{\arg\min}\ \sigma_{I,\mathrm{SML}}^2. \tag{46}$$

For the case of $M > L$, the steps of finding the optimum spreading factor are the same as the ones for the case of $M \leq L$, except for modifying (43) and (45) as follows:

$$\sigma_{I,\mathrm{SML}}^2 = E_S\left[\frac{2}{L}\left(M - L + \frac{L-1}{M} + K - 1\right) + \frac{7L^2}{3}(\pi f_D T_C)^2 \sigma_0^2\right] \tag{47}$$

$$L_{\mathrm{opt}} = \left(\frac{3}{7} \cdot \frac{M - 1/M + K - 1}{(\pi f_D T_C)^2 \sigma_0^2}\right)^{1/3}. \tag{48}$$

The above modification is made by considering the worst case of $M > L$, i.e., $M = \lambda L$ and $\sigma_m^2 = 1/M$ for $0 \leq m \leq M-1$. Indeed, given the system and channel parameters, by using (45), (46), and (48), one can easily determine the optimum spreading factor $L_{\mathrm{opt}}^{\mathrm{SML}}$ for the RBSC system employing the SML detector.

VI. Numerical Results

The performances of the single-input–single-output (SISO) and 2ISO DS-CDMA systems are evaluated with the channel models specified in the UMTS standard [17]. For all numerical results, the carrier frequency and system bandwidth are 2.1 GHz and 3.84 MHz, respectively, and the modulation is BPSK. In addition, we consider the channel assumptions given in Section II-B and employ the typical urban (TU120) and hilly terrain (HT120) channel models [17] with the mobile speed of 120 km/h and the time resolution of $T_C = 0.26\ \mu$s. The numbers of paths (M) for the TU120 and HT120 channel models

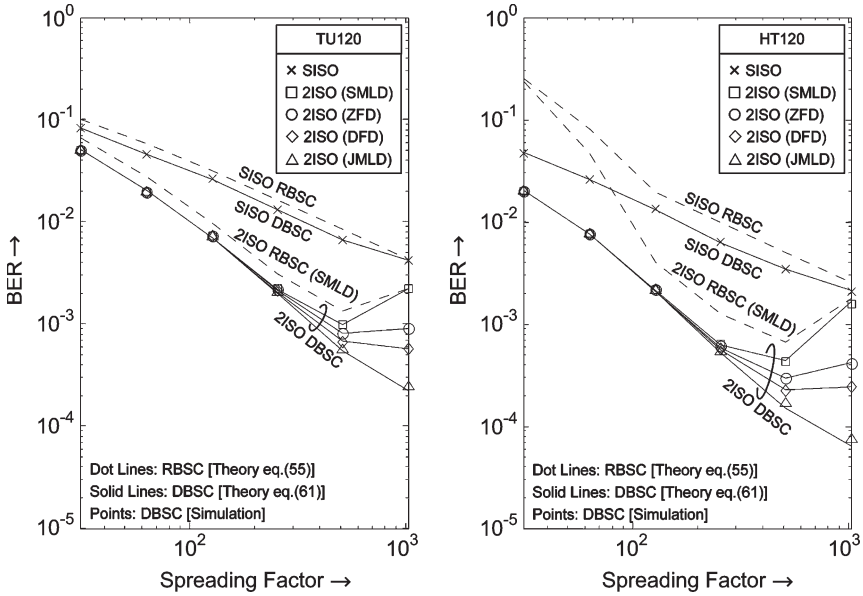

Fig. 3. BER versus L for $K = 5$ and $E_S/N_0 = \infty$.

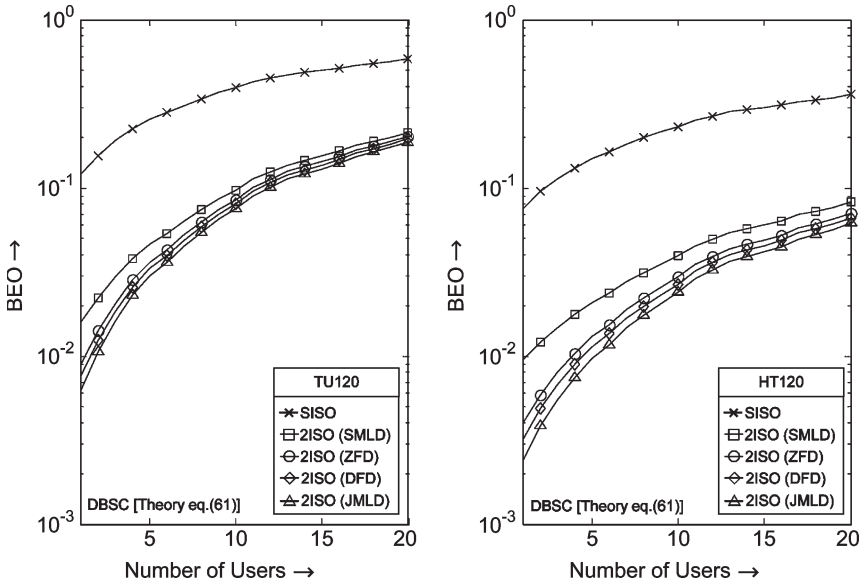

Fig. 4. BEO versus K for $L = 511$, $E_S/N_0 = 25$ dB, and $P_{\rm th} = 3 \times 10^{-2}$.

are nine and 70, respectively. Subsequently, the DBSC systems using Gold codes [14] are considered, and their averaged BERs and BEOs over all users are presented.

Fig. 3 shows the analytical error floors corresponding to a set of spreading factors $\mathcal{L} = \{31, 63, 127, 255, 511, 1023\}$ for the case of $K = 5$. The SISO RBSC system and the 2ISO RBSC system using the SML detector are treated as the baseline systems, and only their theoretical BERs are illustrated. One should note that for the TU120 channel model, the number of previous symbols resulting in ISI is $N = 1$ if $L \in \mathcal{L}$. However, for the HT120 channel model, we have 1) $N = 3$ if $L = 31$; 2) $N = 2$ if $L = 63$; and 3) $N = 1$ if $L \in \{127, 255, 511, 1023\}$. As discussed in Section IV, it is the MPI, MUI, and crosstalk that cause the error floors. For the DBSC systems, the JML detector, being robust to the crosstalk, obtains the best performance, while the SML detector, ignoring the crosstalk, obtains the worst performance. Moreover, increasing L has three impacts on the system performance. First, the power of the total interference $2(\sigma_P^2 + \sigma_S^2 + \sigma_U^2)$ decreases, and hence, all error floors are lower. This evidences that the interference-rejection ability of a DS-CDMA system can be enhanced by increasing L. Second, the power of the crosstalk $\sigma_H^2 E_S(1 - \rho_t^2)$ increases, and thus, the error floors of the 2ISO DS-CDMA systems without employing the JML detector become higher. Finally, the data rate $1/T_S$ decreases. Therefore, a moderate L should be chosen based on the specific channel condition and system requirements.

In the light of (45), (46), and (48), for both TU120 and HT120 channel models, the optimum spreading factor of the 2ISO RBSC system using the SML detector is $L_{\rm opt}^{\rm SML} = 511$. This can be easily verified from Fig. 3. In addition, one can find that $L_{\rm opt}^{\rm SML}$ is a good estimate of the optimum spreading factors for DBSC systems utilizing the SML, ZF, and DF detectors. Indeed, $L_{\rm opt}^{\rm SML}$ is very useful in determining system parameters.

To provide a more objective judgment on the transmission quality within a fading environment, Fig. 4 illustrates the theoretical BEOs of

DBSC systems corresponding to different number of users for $L = 511$, $E_S/N_0 = 25$ dB, and the target BER being $P_{\text{th}} = 3 \times 10^{-2}$. Here, we define the system capacity as the number of users for which the BEO is smaller than 4%. Then, for the TU120 channel model, the system capacities are approximately four, five, six, and seven users, respectively, for the SML, ZF, DF, and JML detectors. On the other hand, for the HT120 channel model, the system capacities are ten, 12, 13, and 14 users, respectively, for the SML, ZF, DF, and JML detectors.

VII. Conclusion

The impacts of a time-varying multipath channel on the performance of the 2ISO STBC-DS-CDMA systems employing various detectors are addressed. The ZF and DF detectors have suboptimum performances but moderate computational complexities and, thus, are recommended for practical implementations. For both RBSC and DBSC systems, with the derived statistical properties of the MD and the interferences, we determine their ESNRs and give their theoretical BERs for time-varying multipath Rayleigh fading channels. Also, we present the theoretical BEOs and evaluate the system capacities. Furthermore, we derive an optimum spreading factor for the RBSC system using the SML detector. Numerical results have revealed that the derived optimum spreading factor is a good estimate of the ones for the DBSC systems using the SML, ZF, and DF detectors. Therefore, it is very useful for system designers in determining the system parameters.

Appendix A
Correlation and Variance of MD

From (11), the correlation of the MD is derived as [13]

$$\rho_H(\Delta i) = \mathrm{E}\left[H_{i+\Delta i}^{(g)} H_i^{(g)*}\right] = \frac{\sigma_0^2}{L^2} \sum_{l=-L+1}^{L-1} (L - |l|)\, J_0\left[2\pi f_D T_C(\Delta i \cdot L + l)\right] \quad (49)$$

and its variance is $\sigma_H^2 = \rho_H(0)$. Also, its normalized correlation of adjacent symbol durations is defined as $\rho_t \triangleq \rho_H(1)/\sigma_0^2$.

Appendix B
Variances of the Interferences for RBSC

From (12) and (13), assuming that information symbols, tap coefficients, and random spreading sequences are mutually independent, one can calculate the variances of the IPI and ISI as follows:

$$\sigma_P^2 = E\left[\left|P_i^{(g)}\right|^2\right] = \frac{E_S}{L^2}\left(L \sum_{m=1}^{\kappa(0)-1} \sigma_m^2 - \sum_{m=1}^{\kappa(0)-1} m\sigma_m^2\right) \quad (50)$$

$$\sigma_S^2 = E\left[\left|S_i^{(g)}\right|^2\right] = \frac{E_S}{L^2}\left(L \sum_{n=1}^{\lambda-1} \kappa(n) + \sum_{m=1}^{\kappa(0)-1} m\sigma_m^2\right). \quad (51)$$

Accordingly, summing up (50) and (51) yields the variance of the MPI as

$$\sigma_P^2 + \sigma_S^2 = \frac{E_S}{L}\left(\sum_{m=1}^{\kappa(0)-1} \sigma_m^2 + \sum_{n=1}^{\lambda-1} \kappa(n)\right). \quad (52)$$

By considering the worst case, namely, $M\lambda = L$ and $\sigma_m^2 = 1/M$ for $0 \le m \le M-1$, its upper bound is obtained as

$$\sigma_P^2 + \sigma_S^2 < \begin{cases} \frac{E_S}{L}, & \text{if } M \le L \\ \frac{E_S}{L}(M - L + 1), & \text{if } M > L\,. \end{cases} \quad (53)$$

From (14), the variance of the MUI can be derived as

$$\sigma_U^2 = E\left[\left|U_i^{(g)}\right|^2\right] = \frac{E_S}{L} \sum_{k=1}^{K-1} \sum_{n=0}^{\lambda-1} \sum_{m=0}^{\kappa(n)-1} \sigma_{m+nL}^2 = \frac{E_S}{L}(K-1). \quad (54)$$

Finally, the power of the total interference is

$$\sigma_P^2 + \sigma_S^2 + \sigma_U^2 = \frac{E_S}{L}\left(\sum_{m=1}^{\kappa(0)-1} \sigma_m^2 + \sum_{n=1}^{\lambda-1} \kappa(n) + K - 1\right) \quad (55)$$

and hence, its upper bound is

$$\sigma_P^2 + \sigma_S^2 + \sigma_U^2 < \begin{cases} \frac{E_S}{L}K, & \text{if } M \le L \\ \frac{E_S}{L}(M - L + K), & \text{if } M > L\,. \end{cases} \quad (56)$$

Thereupon, if $M \le L$, the total interference can be approximated as the MUI contributed by K users. This confirms the assumption in [5], where the case of $M < L$ is considered. However, if $M > L$, the total interference should be approximated as the MUI contributed by $M - L + K$ users. Indeed, from (56), it is evident that the number of paths M and the number of users K dominate the quantity of the total interference while the spreading factor L stands for the inherent interference-rejection ability of a DS-CDMA system.

Appendix C
Variances of the Interferences for DBSC

From (12) and (13), for deterministic spreading, assuming that the information symbols and channel-tap coefficients are independent, one can derive the variances of the IPI and ISI as

$$\sigma_P^2 = E\left[\left|P_i^{(g)}\right|^2\right] = E_S \sum_{m=0}^{\kappa(0)-1} \sigma_m^2 \sum_{l=m}^{L-1} \sum_{l'=m}^{L-1} J_0\left[2\pi f_D T_C(l-l')\right] \times b_{0,l-m} b_{0,l'-m} b_{0,l} b_{0,l'} - E_S \sigma_H^2 \quad (57)$$

$$\sigma_S^2 = E\left[\left|S_i^{(g)}\right|^2\right] = E_S \sum_{n=1}^{\lambda-1} \sum_{m=0}^{\kappa(n)-1} \sigma_{m+nL}^2 \sum_{l=m}^{L-1} \sum_{l'=m}^{L-1} J_0\left[2\pi f_D T_C(l-l')\right] \times b_{0,l-m} b_{0,l'-m} b_{0,l} b_{0,l'} + E_S \sum_{n=0}^{\lambda-1} \sum_{m=1}^{\kappa(n)-1} \sigma_{m+nL}^2 \times \sum_{l=0}^{m-1} \sum_{l'=0}^{m-1} J_0\left[2\pi f_D T_C(l-l')\right] b_{0,l-m+L} b_{0,l'-m+L} b_{0,l} b_{0,l'}. \quad (58)$$

Thus, the variance of the MPI is

$$\sigma_P^2+\sigma_S^2=E_S\sum_{n=0}^{\lambda-1}\sum_{m=0}^{\kappa(n)-1}\sigma_{m+nL}^2\times\left(\sum_{l=m}^{L-1}\sum_{l'=m}^{L-1}J_0\left[2\pi f_DT_C(l-l')\right]b_{0,l-m}b_{0,l'-m}b_{0,l}b_{0,l'}+\sum_{l=0}^{m-1}\sum_{l'=0}^{m-1}J_0\left[2\pi f_DT_C(l-l')\right]\times b_{0,l-m+L}b_{0,l'-m+L}b_{0,l}b_{0,l'}\right)-E_S\sigma_H^2. \quad (59)$$

From (14), the variance of the MUI is derived as

$$\sigma_U^2=E\left[\left|U_i^{(g)}\right|^2\right]=E_S\sum_{k=1}^{K-1}\sum_{n=0}^{\lambda-1}\sum_{m=0}^{\kappa(n)-1}\sigma_{m+nL}^2\times\left(\sum_{l=m}^{L-1}\sum_{l'=m}^{L-1}J_0\left[2\pi f_DT_C(l-l')\right]b_{k,l-m}b_{k,l'-m}b_{0,l}b_{0,l'}+\sum_{l=0}^{m-1}\sum_{l'=0}^{m-1}J_0\left[2\pi f_DT_C(l-l')\right]\times b_{k,l-m+L}b_{k,l'-m+L}b_{0,l}b_{0,l'}\right). \quad (60)$$

Finally, adding up (59) and (60) yields the power of the total interference as

$$\sigma_P^2+\sigma_S^2+\sigma_U^2=E_S\sum_{k=0}^{K-1}\sum_{n=0}^{\lambda-1}\sum_{m=0}^{\kappa(n)-1}\sigma_{m+nL}^2\times\left(\sum_{l=m}^{L-1}\sum_{l'=m}^{L-1}J_0\left[2\pi f_DT_C(l-l')\right]b_{k,l-m}b_{k,l'-m}b_{0,l}b_{0,l'}+\sum_{l=0}^{m-1}\sum_{l'=0}^{m-1}J_0[2\pi f_DT_C(l-l')]\times b_{k,l-m+L}b_{k,l'-m+L}b_{0,l}b_{0,l'}\right)-E_S\sigma_H^2. \quad (61)$$

For the static channel, i.e., $f_D=0$, (61) is reduced to

$$\sigma_P^2+\sigma_S^2+\sigma_U^2=E_S\sum_{k=0}^{K-1}\sum_{n=0}^{\lambda-1}\sum_{m=0}^{\kappa(n)-1}\sigma_{m+nL}^2\times\left[\left(\sum_{l=m}^{L-1}b_{k,l-m}b_{0,l}\right)^2+\left(\sum_{l=0}^{m-1}b_{k,l-m+L}b_{0,l}\right)^2\right]-E_S\sigma_0^2 \quad (62)$$

which is of much lower computational complexity. According to extensive computer simulations in which the well-designed pseudo-random codes, having good automatic and cross-correlation properties (e.g., Gold codes and Kasami codes [14]), were used as spreading sequences, we found that (62) is a good approximation of (61) as long as $f_DT_C<0.0025$.

REFERENCES

[1] S. M. Alamouti, "A simple transmit diversity scheme for wireless communications," *IEEE J. Sel. Areas Commun.*, vol. 16, no. 8, pp. 1451–1458, Oct. 1998.

[2] A. Vielmon, Y. Li, and J. R. Barry, "Performance of Alamouti transmit diversity over time-varying Rayleigh-fading channels," *IEEE Trans. Wireless Commun.*, vol. 3, no. 5, pp. 1369–1373, Sep. 2004.

[3] Z. Liu, X. Ma, and G. B. Giannakis, "Space-time coding and Kalman filtering for time-selective fading channels," *IEEE Trans. Commun.*, vol. 50, no. 2, pp. 183–186, Feb. 2002.

[4] K. S. Ahn and H. K. Baik, "Performance improvement of space-time block codes in time-selective fading channels," *IEICE Trans. Commun.*, vol. E87-B, no. 2, pp. 364–368, Feb. 2004.

[5] T. Eng and L. Milstein, "Coherent DS-CDMA performance in Nakagami multipath fading," *IEEE Trans. Commun.*, vol. 43, no. 2–4, pp. 1134–1143, Feb.–Apr. 1995.

[6] *Physical Channels and Mapping of Transport Channels Onto Physical Channels (FDD) (3GPP TS 25.211)*, Dec. 2005.

[7] R. T. Derryberry, S. D. Gray, D. M. Ionescu, G. Mandyam, and B. Raghothaman, "Transmit diversity in 3G CDMA systems," *IEEE Commun. Mag.*, vol. 40, no. 4, pp. 68–75, Apr. 2002.

[8] R. A. Soni and R. M. Buehrer, "On the performance of open-loop transmit diversity techniques for IS-2000 systems: A comparative study," *IEEE Trans. Wireless Commun.*, vol. 3, no. 5, pp. 1602–1615, Sep. 2004.

[9] B. A. Bjerke, Z. Zvonar, and J. G. Proakis, "Antenna diversity combining schemes for WCDMA systems in fading multipath channels," *IEEE Trans. Wireless Commun.*, vol. 3, no. 1, pp. 97–106, Jan. 2004.

[10] X. Wang and J. Wang, "Effect of imperfect channel estimation on transmit diversity in CDMA systems," *IEEE Trans. Veh. Technol.*, vol. 53, no. 5, pp. 1400–1412, Sep. 2004.

[11] J. Jootar, J. R. Zeidler, and J. G. Proakis, "Performance of Alamouti space-time code in time-varying channels with noisy channel estimates," in *Proc. IEEE Wireless Commun. Netw. Conf.*, Mar. 2005, pp. 498–503.

[12] A. Conti, M. Z. Win, M. Chiani, and J. H. Winters, "Bit error outage for diversity reception in shadowing environment," *IEEE Commun. Lett.*, vol. 7, no. 1, pp. 15–17, Jan. 2003.

[13] D. B. Lin, P. H. Chiang, and H. J. Li, "Performance analysis of two-branch transmit diversity block coded OFDM systems in time-varying multipath Rayleigh fading channels," *IEEE Trans. Veh. Technol.*, vol. 54, no. 1, pp. 136–148, Jan. 2005.

[14] G. L. Stüber, *Principles of Mobile Communication*, 2nd ed. London, U.K.: Kluwer, 2001.

[15] C. E. Shannon, "Communication in the presence of noise," *Proc. IRE*, vol. 37, no. 1, pp. 10–21, Jan. 1949.

[16] I. S. Gradshteyn and I. M. Ryzhik, *Table of Integral, Series, and Products*, 6th ed. London, U.K.: Kluwer, 2000.

[17] *Deployment Aspects (3GPP TR 25.943)*, Dec. 2004.